BBA - Biomembranes 1865 (2023) 184160

Contents lists available at ScienceDirect

BBA - Biomembranes

journal homepage: www.elsevier.com/locate/bbamem

Analyzing mechanisms of action of antimicrobial peptides on bacterial membranes requires multiple complimentary assays and different bacterial strains

Xiaoqi Wang [a], Roy A.M. van Beekveld [a], Yang Xu [a], Anish Parmar [c,d], Sanjit Das [c,d], Ishwar Singh [c], Eefjan Breukink [a,b,*]

[a] Membrane Biochemistry and Biophysics, Department of Chemistry, Faculty of Science, Utrecht University, Utrecht, Netherlands
[b] Zhejiang Provincial Key Laboratory of Food Microbiotechnology Research of China, the Zhejiang Gongshang University of China, Hangzhou, China
[c] Antimicrobial Pharmacodynamics and Therapeutics, Department of Pharmacology and Therapeutics, Institute of Systems, Molecular & Integrative Biology, University of Liverpool, William Henry Duncan Building, 6 West Derby St, Liverpool L7 8TX, UK
[d] Antimicrobial Drug Discovery and Development, Department of Chemistry, The Robert Robinson Laboratories, University of Liverpool, L69 3BX Liverpool, UK

ARTICLE INFO

Keywords:
Antimicrobial peptides
Membrane effects
Membrane potential
pH homeostasis
ATP homeostasis

ABSTRACT

Antimicrobial peptides (AMPs) commonly target bacterial membranes and show broad-spectrum activity against microorganisms. In this research we used three AMPs (nisin, epilancin 15×, [R4L10]-teixobactin) and tested their membrane effects towards three strains (*Staphylococcus simulans*, *Micrococcus flavus*, *Bacillus megaterium*) in relation with their antibacterial activity. We describe fluorescence and luminescence-based assays to measure effects on membrane potential, intracellular pH, membrane permeabilization and intracellular ATP levels. The results show that our control peptide, nisin, performed mostly as expected in view of its targeted pore-forming activity, with fast killing kinetics that coincided with severe membrane permeabilization in all three strains. However, the mechanisms of action of both Epilancin 15× as well as [R4L10]-teixobactin appeared to depend strongly on the bacterium tested. In certain specific combinations of assay, peptide and bacterium, deviations from the general picture were observed. This was even the case for nisin, indicating the importance of using multiple assays and bacteria for mode of action studies to be able to draw proper conclusions on the mode of action of AMPs.

1. Introduction

Antimicrobial resistance is becoming a global threat to human health as more and more antibiotics are losing their efficacy. Antimicrobial peptides (AMPs) showing broad-spectrum activity against microorganisms have been considered already for a long time as promising substitutions for these antibiotics [1–3]. AMPs are mostly positively charged and amphiphilic, properties that are essential for their (initial) interaction with the negatively charged membranes of target bacteria [4]. Currently, there are three main models that are describing the possible mechanisms of action of AMPs, i.e., the barrel-stave model, carpet model and toroidal-pore model [4–6]. However, these three classic models cannot account for the modes of action of many AMPs. In addition, mechanisms of actions are often ascribed to peptides while using improper model systems (e.g. composed of only one lipid) [6,7]. Increasingly more models have been proposed by which AMPs destabilize the target membrane. Examples of these are thinning of the membrane, clustering of anionic lipids or non-lytic membrane depolarization [8–11]. Alternatively, the AMPs induce phase separations that lead to destabilization of the bacterial membranes via blebbing, budding, or vascularization [12–15]. Recently, it was shown that many AMPs lacked a correlation between membrane permeabilization and antibiotic activity. This led to the suggestion that these AMPs inhibit bacteria by perturbating the membrane and causing intracellular biomass aggregation [16]. What all AMPs have in common is their affinity for the bacterial membrane, and even those that have internal targets but do not cause permeabilization have mechanisms to pass this membrane that are similar to certain pore-forming mechanisms [16]. Importantly, what mechanism a peptide is proposed to follow largely depends on the method and bacterium used for determining the

* Corresponding author at: Membrane Biochemistry and Biophysics, Z807, Padualaan 8, 3584 CH Utrecht, Netherlands.
E-mail address: e.j.breukink@uu.nl (E. Breukink).

https://doi.org/10.1016/j.bbamem.2023.184160
Received 21 November 2022; Received in revised form 21 March 2023; Accepted 3 April 2023
Available online 24 April 2023

peptide's effects [17,18]. Thus, the way in which membrane permeabilization by an AMP is determined has major implications for the conclusions that can (and will) be drawn on the proposed mechanism.

AMPs' effects on bacterial membranes can be subtle, such as membrane depolarization or more severe, like pore-formation or disruption via the carpet model and several methods exist that can measure these effects on membranes. Dissipation of the membrane potential (ΔΨ) and/or ΔpH, are the subtlest indications of membrane perturbation that can be measured. Both constitute the so-called proton-motive force (PMF, Δp) where $\Delta p = \Delta\psi - 2.3RT / F * \Delta pH$ [19]. The dissipation of the PMF is triggered by proton leakage or membrane potential depolarization (ion leakage, in case of bacteria mostly K^+). The depolarization of the membrane can be measured by voltage-sensitive cyanine dyes such as 3,3′-Diethylthiadicarbocyanine ($DisC_2(5)$) [20–23]. In the presence of a membrane potential, these dyes are absorbed into the bilayer and accumulate presumably in the inner leaflet of the plasma membrane resulting in self-quenching [24]. The dyes are released after depolarization of the membrane and as a result the self-quenching is relieved [25–27]. Changes in the pH gradient are mostly measured by determining the pH of the cytosol via internalized pH-sensitive fluorophores. Carboxyfluorescein diacetate succimidyl ester can be used for this, where its esterized form can enter the cell and following de-esterification it becomes fluorescent [28]. The succimidyl ester ensures stable intracellular localization. Besides dissipation of the PMF due to loss of ions or proton influx, more severe membrane damage, such as pore-formation, can be measured by determining the efflux of (much) larger intracellular components. The earliest method used for this was detecting the release of UV-absorbing components of the cell [29]. In addition, the loss of ATP by the cells can be determined by a luciferase based assay [30]. An alternative way to determine the membrane damage is using probes that can enter the cells when their membrane is damaged. DNA-binding probes such as SYTOX green or 4′,6-diamidino-2-phenylindole (DAPI) are membrane impermeable and they stain the DNA only when the membrane barrier is compromised [31–38].

Members of the family of lantibiotics, which belongs to AMPs, usually have specific mechanisms and large amount of them harbors the Lipid II targeting family members [39,40]. Nisin (Fig. S1A) is one of the most well studied member of the lantibiotics family that targets Lipid II and forms stable pores together with Lipid II in the bacterial membrane [17,41–43]. The A and B ring-system of nisin is responsible for binding to Lipid II and the C-terminal part of nisin including rings D/E has been suggested to be important for pore-formation [44]. A recent high-resolution NMR study revealed more details on the nisin-Lipid II binding in membrane bilayers, where the N20-K22 (the hinge) of nisin was shown to be flexible and lines the pore lumen. This was suggested to be important for the adaption of the pores to the thickness of the membrane [45]. The C-terminal (S29-K34) part of nisin was shown to still be dynamic in the pore structure and it is proposed to pierce through the membrane [45]. Pores formed by nisin are very stable and black lipid bilayer studies have shown that nisin pores have a pore-size of about 2 to 2.5 nm, thus allowing molecules the size of ATP (Stokes radius of ~0.7) through the pore [43,46]. The mode of action of epilancin 15× (Fig. S1B), another member of the lantibiotics family, is still unknown. Therefore we aimed to study the antibacterial activity of this peptide in comparison to nisin. Epilancin 15×, which has one of the lowest MICs against pathogenic bacteria and has potent activity especially against Staphylococci [47]. It is produced by *Staphylococcus epidermidis* 15 × 154 and was isolated and structurally characterized in 2005 [48]. The C-terminus of epilancin 15×, especially rings B and C, is very similar to nisin, which may point to pore-formation as its mechanism [47]. However, epilancin 15× lacks nisin's N-terminal lipid II signature binding A/B rings system, which makes it uncertain if it interacts with Lipid II. As mentioned, how epilancin 15× acts is still unclear, but given the similarity of the C-terminal lanthionine rings it may, like nisin, attack bacteria via membrane permeabilization. Teixobactin, which is produced by *Eleftheria terrae*, kills pathogens via targeting Lipid II and the wall teichoic acid precursor Lipid III, thus its mode of action includes inhibition of the bacterial cell wall synthesis machinery [49]. Recently it was shown that teixobactin has a dual mode of action that besides cell wall synthesis inhibition also includes membrane disruption via fibril formation together with Lipid II on the membrane surface [50]. This aggregational behavior with Lipid II had been shown before for an improved teixobactin analog, D-Arg4-Leu10-teixobactin ([R4L10]-teixobactin, Fig. S1C) [51,52]. Hence, we also explored the permeabilization activity of this teixobactin analog compared to that of nisin and epilancin 15×.

During our efforts in studying the membrane effects of these AMPs we noticed that even a well-known pore-former, the lantibiotic nisin, sometimes behaved differently from what can be expected from a pore-forming peptide in different methods and bacteria. Our results indicate that it is important to use multiple assays and bacteria for mode of action studies to be able to draw proper conclusions on the mode of action of AMPs.

2. Method and materials

2.1. Materials and strains

Nisin A, epilancin 15× were prepared as previously described [48,53]. [R4L10]-teixobactin was obtained from Ishwar Singh (University of Liverpool). 3,3′-Diethylthiadicarbocyanine iodide ($DiSC_2(5)$), 4′,6-diamidino-2-phenylindole (DAPI) and Triton X-100 were purchased from Sigma-Aldrich. SYTOX™ Green Nucleic Acid Stain (SYTOX green) and 5(6)-CFDA, SE, Luria Broth (LB) and Tryptone Soya Broth (TSB) were purchased from ThermoFisher. M9 medium supplemented with vitamins and salts was prepared as described [54]. BacTiter-Glo™ Microbial Cell Viability Assay Kit was purchased from Promega. All other chemicals or reagents used were of analytical grade. Strains used in this study: *S. simulans* 22 [55]; *M. flavus* DSM 1790; *B. megaterium* ATCC 14581.

2.2. Methods

2.2.1. General procedures

Precultures of the indicator strains were grown at 37 °C in TSB for *S. simulans* and *M. flavus* or LB for *B. megaterium* while shaking at 200 rpm overnight and then diluted to an OD_{600} of 0.05 with fresh medium. The cultures were further grown for 4 h and spun down at 3000 ×*g* for 10 min at 4 °C. The cells were washed twice with buffer A (250 mM glucose, 5 mM $MgSO_4$, 100 mM KCl, 10 mM potassium-phosphate buffer at pH 7) for *S. simulans* and *M. flavus* or M9 medium for *B. megaterium*. They were then resuspended to an OD_{600} of 5 and kept on ice until use on the same day. The bacteria remained viable under these conditions for at least 2 h.

The concentration of peptides was determined using the Pierce™ BCA Protein Assay Kit (Thermo Fisher) using BSA as a standard. Fluorescence and luminescence related experiments (membrane potential depolarization assay, membrane permeability assay, ATP leakage assay, proton permeability assay) were performed using a Cary Eclipse fluorescence spectrophotometer (FL0904M005) in a 10 × 4-mm quartz cuvette at 25 °C.

To determine the number of surviving cells in the fluorescence cuvette at a given time, 5 μL of the suspension was plated onto TSB agar plates and incubated at 37 °C overnight.

Per species of bacteria all the experiments were done on the same day and due to time restraints, per experiment, one set of data could only be obtained. For each bacterium this was repeated at least twice, thus generating fully independent measurements.

2.2.2. MIC determination

The lowest concentrations of AMPs (nisin, epilancin 15× and teixobactin) that did not allow growth of the indicator strains after 18 h

were defined as the MICs. This was determined using 1 mL cultures of indicator strains at a start OD_{600} of 0.05 in fresh medium (TSB for *S. simulans* and *M. flavus* or LB for *B. megaterium*) containing a serial dilution of antibiotics in sterilized glass tubes. The tubes were shaken at 37 °C, 200 rpm and the OD_{600} was determined after incubation for 18 h on a Novaspec II. MIC determination were repeated three times.

2.2.3. Membrane potential depolarization assay

The fluorescent dye $DiSC_2(5)$ (excitation at 650 nm and emission at 670 nm) was used to test the effect of the antibiotics on the membrane potential of the bacteria. From the concentrated cell suspension, cells were diluted to $OD_{600} = 0.05$ in a cuvette containing 1 mL of buffer A, followed by the addition of 2 μL of a stock solution of 0.1 mM $DiSC_2(5)$ dissolved in DMSO. Antibiotics were added after 1 min, or left out for the blank. At the end of the experiment 10 μL of 20 % Triton X-100 was added to fully dissipate the membrane potential.

2.2.4. Membrane permeability assay (DNA binding stain)

The fluorescent dyes SYTOX green (excitation at 504 nm and emission at 523 nm) and DAPI (excitation at 364 nm and emission at 454 nm) were used to inspect the abilities of the antibiotics to disrupt the bacterial membrane. From the concentrated cell suspension 10 μL was added into a cuvette containing 1 mL buffer A to reach an OD_{600} of 0.05, followed by the addition of 1 μL of a stock solution of 0.25 μM SYTOX green dissolved in DMSO or 1 μL of a stock solution of 1 mg/mL DAPI dissolved in 10 mM PBS at pH 7. Antibiotics were added after 1 min, or left out for the blank. At the end of the experiment 10 μL of 20 % Triton X-100 for SYTOX green or BacTiter-Glo™ disruption buffer for DAPI was added to fully disrupt the cells.

2.2.5. ATP leakage assay

The BacTiter-Glo™ Microbial Cell Viability Assay Kit was used to inspect the abilities of the antibiotics to cause ATP leakage from the bacteria. Luciferase signal was recorded using the Bio/Chemiluminescence mode with the emission set at 556 nm. The BacTiter-Glo™ substrate stock solution containing the luciferase enzyme and substrate was made by dissolving the lyophilized substrate/enzyme mixture provided in the kit in 1 mL of buffer A, which was then divided into 50 μL aliquots and stored at −80 °C until use. From the concentrated cell suspension 10 μL was added into a cuvette containing 1 mL buffer A, followed by the addition of 5 μL of BacTiter-Glo™ substrate solution. Antibiotics were added after 1 min, or left out for the blank. At the end of the experiment 10 μL of BacTiter-Glo™ disruption buffer was added to measure the amount of residual ATP that was left inside the cells. Experiments using *B. megaterium* were performed in M9 medium to maintain viability of the cells. Unfortunately, ATP measurements were incompatible with M9 medium.

2.2.6. Proton permeability assay

The 5(6)-CFDA, SE (excitation at 490 nm and emission at 525 nm) was used to inspect the proton permeabilities of the antibiotics against the bacteria. Precultures of indicator strains were grown at 37 °C, 200 rpm overnight, and then diluted to an OD_{600} of 0.05 with fresh medium. The culture was further grown for 4 h and spun down at 3000 ×*g* for 10 min at 4 °C. Then cells were resuspended in buffer B containing 50 mM HEPES, 20 mM glucose, 1 mM $MgSO_4$ at pH 7 to an OD_{600} of 0.5 and incubated with 3 μM 5(6)-CFDA, SE for 30 min at 30 °C, 200 rpm. The cells were washed twice with the same buffer and were resuspended to an OD_{600} of 5. From this cell suspension 10 μL was added into a cuvette containing 1 mL buffer B set at pH 5. Antibiotics were added after 30 s, or left out for the blank. At the end of the experiment 20 μL of a 1 mg/mL carbonyl cyanide *m*-chlorophenyl hydrazone (CCCP) solution in DMSO was added to fully dissipate the ΔpH of the bacteria.

2.2.7. Analysis of lipid compositions of bacteria

Bacteria were grown overnight at 37 °C while shaking @200 rpm in TSB in the case of *S. simulans*, or at 30 °C while shaking at 200 RPM for *B. megaterium* (in LB) and *M. flavus* (in TSB). The overnight culture was diluted to an OD_{600} of 0.05 in 10 mL and grown to mid-log phase (OD_{600} = 0.3–0.4) at the same conditions as for the overnight growth. Bacteria were harvested, resuspended in 0.8 mL H_2O, after which 2 mL MeOH and 1 mL $CHCl_3$ were added and the samples were vortexed extensively. Subsequently, 1 mL of $CHCl_3$ and H_2O were added, the sample vortexed and then centrifuged at 1000 ×*g* for 2 min. The organic layer (bottom) was dried under a N_2 stream at 40 °C. The dried lipids were weighed and redissolved in 250 μL 2:1 $CHCl_3$:MeOH. Lipids were then spotted onto a NP-TLC (HPTLC-Fertigplatten Nano-ADAMANT®) at 20 μg total lipids per lane using a Camag Linomat 5. The TLC was developed in 48:48:3:1, $CHCl_3$:EtOH:NH_3:H_2O with 0.2 g/L NH_4Ac, dried under vacuum and then stained with iodine prior to imaging. Phospholipid species were assigned based on pure references and the bacterial lipid extracts were analyzed as three independent cultures per species.

For analysis of the acyl chain compositions, approximately 1 mg of the bacterial extracts were redissolved in 1 mL n-hexane. Subsequently, 200 μL MeOH containing 100 g/L KOH was added and the samples were extensively vortexed for 1 min to obtain fatty acid methyl esters (FAMEs). The n-hexane layer was taken, dried under a N2-stream and redissolved in 50 μL n-hexane. The FAMEs were then analyzed using gas chromatography with flame-ionization detection on a Trace GC Ultra (Thermo Fisher Scientific) equipped with a biscyanopropyl polysiloxane column (Restek) and N2 as a carrier gas. A temperature gradient was used that started at 40 °C and held for 1 min, followed by a linear gradient to 160 °C in 4 min and a subsequent linear gradient to 220 °C in 15 min. Peak identification was performed using FAME standards Mixture BR2 (Larodan; 90-1052) for branched species and certain straight chain fatty acids or 63-B (Nu-Chek-Prep) for various unsaturated and straight chain fatty acid species.

3. Results

The peptides under study here are targeted. Hence, to ensure that unspecific (non-targeted) mechanisms do not play a role we deliberately selected strains with low MICs to avoid clouding the results with a-specific effects.

3.1. Nisin causes severe membrane disruption in S. simulans and B. megaterium typical for pore-formation

Nisin displayed MIC values equal to 80 nM, 50 nM and 75 nM towards *S. simulans*, *M. flavus* and *B. megaterium* respectively. In general, severe membrane disruption, e.g. pore-formation, of a bacterium leads to rapid death. This fast-killing rate should also correspond to the effects observed in the assays that are employed to determine membrane effects of AMPs if their mode of action involves membrane disruption. Therefore, we also determined the number of cells killed by nisin by determining the amount of colony forming units (CFU) after 5 min incubation, the average time needed for the assays employed here, at the different concentrations mentioned above. To exclude any environmental influence on the results we determined the CFUs that are present in the same cuvette and under the identical conditions used for the fluorescence experiments. From these plate assays it becomes clear that nisin is able to kill rapidly, as can be expected from its targeted pore-forming mechanism. At 5× and 10× MIC there is about a 3 and 4 log reduction respectively in viable cells after 5 min and after 1 min already more than 99 % of the bacteria have been killed (Fig. P1). At lower nisin concentrations (1× and 2× MIC) only a 1 or 2 log reduction was achieved in 5 min and killing clearly takes longer.

The activity of AMPs, expressed in their MIC-values, towards different strains and in comparison to others can vary quite extensively from nanomolar to micromolar values depending on the killing mechanism they use. Therefore, in order to allow easy comparison, we used AMP-concentrations equal to 1×, 2×, 5× and 10× the respective MICs of

the different strains in all the assays that report on membrane effects by the AMPs.

When testing the effects of nisin on the membrane potential with the dye $DiSC_2(5)$ or the effect on membrane permeability to a DNA probe with the dye Sytox green/DAPI, in all cases, a picture emerges where the membrane effects parallel the killing rates (Figs. 1A, B and S2A). At low MICs relative minor effects can be seen, while at the highest concentrations (5× and 10× MIC) the effects are maximal of what can be achieved in the assay. The ΔpH measurements deviate from this picture where already a maximum effect was achieved with a concentration of only 1× MIC in about 1 min (Fig. 1C). An interesting case is presented when we tested for ATP leakage in an on-line assay using luciferase to determine both intra cellular ATP levels as well as ATP-leakage from the cells. As luciferase is unable to enter the cell spontaneously and is too large to leak through the pores formed by nisin, this assay allowed us to determine i) the extent of ATP leakage from the bacteria in time and ii) the total amount of ATP remaining in the bacteria after 5 min of incubation with nisin. The low MIC traces (1× and 2× MIC) are especially interesting as it shows that two simultaneously occurring processes have to be considered (Fig. 1D). The addition on nisin at this concentration clearly induced some leakage of ATP in 5 min, amounting to a little over 10 % of the original amount of ATP in the cells (as deduced from the maximal signal obtained from the blank after lysis of the cells). However, simultaneously the total amount of ATP present in the cells had dropped considerable. Only about 50 % of the ATP was left with respect to the control, meaning that an additional 40 % of ATP was lost somehow. This drop in cellular ATP can be explained by taking into account that, within 1 min, nisin induced a complete dissipation of the ΔpH, the main driving force for the generation of ATP in the bacteria [56]. As all ATP-consuming processes (e.g. protein synthesis, a major ATP-consumer) within the cell are still active, this results in a dramatic drop of the ATP-levels. At the highest concentration of nisin a little over 20 % of the original amount of ATP has leaked out of the cells in 5 min, while nothing remains as there is no extra increase of signal upon complete lysis of the cells. Thus the remaining cells are completely devoid of ATP and have lost their ATP due to the combined losses due to leakage and consumption in the absence of ATP regeneration. So far, studies on luciferase-based ATP determination for cells have been off-line-and only determined the amount of ATP that leaked out after separating the cells from the medium. Our method is able to determine both the amount of ATP leakage in time and the total amount of ATP that is left in the cells at a given timepoint, a valuable improvement of the assay.

We next tested nisin's activity towards *B. megaterium*, a bacterium with a similar sensitivity towards nisin as *S. simulans* (both 75 nM). Surprisingly, *B. megaterium* seemed to be much more sensitive in the membrane disruption assays (even in M9 medium) as its MIC would suggest. Membrane effects could be observed in all assays at concentrations starting 100-fold lower than the MIC, which also correlated with a rapid drop in CFUs at similar concentrations (Fig. P2). Apparently, this bacterium is much more sensitive towards nisin under the conditions of the membrane permeability tests (M9 medium) opposed to MIC tests in growth medium (LB-broth). Yet, at these lower concentrations, a fairly similar behavior of nisin was seen towards *B. megaterium* as compared to *S. simulans* with all membrane disruption assays (Fig. S2E–H). Here, the disruption of the ΔpH was very fast as well and already complete within a minute, but also the membrane-potential measurements showed fast dissipation kinetics. Thus, both the two components of the PMF, ΔΨ and ΔpH, were affected early as compared to the more severe membrane effects measured by the DNA probes. Taken together, the results with these two bacteria show that there is a good correlation between the killing rates observed and the membrane disruption measured by the different assays.[1]

3.2. Deviations from ideal behavior as a pore-former with *M. flavus*

M. flavus is a bit more sensitive to nisin (MIC of 50 nM) as compared to *S. simulans* (75 nM). The killing rate of nisin towards this bacterium is similarly fast as compared to *S. simulans* as at a 10-fold MIC concentration of nisin 3–4 log killing was achieved in 5 min (Fig. P3).

The effects of nisin in the membrane potential assay, Sytox green assay and ATP-leakage assay on *M. flavus*, were all comparable to the effects observed for the other bacteria (Fig. S2B–C and Fig. 1F). Surprisingly, the effects of nisin on the ΔpH of *M. flavus* were much less pronounced. Instead of a rapid decrease of the signal in the first minutes as seen for the other bacteria, a gradual decrease over time was observed (Fig. 1E). This coincided with a low drop of ATP levels within the cells at the lower concentrations, again showing that the ΔpH and the ATP content of the cells are correlated. Importantly, the leakage assay using DAPI was completely non-responsive to the effects of nisin on *M. flavus* (Fig. S2D). Since DAPI is a factor of ~2 times smaller than Sytox green the size of the probe cannot explain this difference in responsiveness. This deviation from the ideal behavior signifies that relying on only one bacterium and one assay for determining membrane effects can be very limiting and can lead to complete misinterpretation of the mode of action. The non-responsiveness of DAPI stands out (also for the other peptides, see below) and makes this probe unsuitable for this kind of membrane permeability assays, at least in combination with *M. flavus*.

3.3. Epilancin 15× does not cause major membrane disruptions in *M. flavus* and *S. simulans*

Epilancin 15× (abbreviated to epilancin) displayed MIC values equal to 100 nM, 75 nM and 100 nM towards *S. simulans*, *M. flavus*, *B. megaterium* respectively. Epilancin behaved quite differently from nisin towards *S. simulans* and *M. flavus*. In contrast to nisin, epilancin was shown to be bacteriostatic towards both *S. simulans* and *M. flavus*; only 1–2 log of cells were killed at the highest concentration (10× MIC) in 5 min (Figs. P4 and P5). The bacteriostatic effect of epilancin towards these strains would suggest that it has less severe membrane perturbing activity. This, we tested using the assays we have validated with nisin as a reference compound above.

First, we used $DiSC_2(5)$ and 5(6)-CFDA, SE to test the membrane depolarization activity and proton permeabilization activity of epilancin towards the two strains. Epilancin causes clear effects in both assays with *S. simulans* that increase with increasing concentration (Fig. 2A and C) albeit that the effects on the ΔpH were not as strong as those of nisin (compare Figs. 1C and 2C). Interestingly, concentrations of epilancin of

[1] Triton X-100 only induced a 100 % effect in the control situation of our Sytox-green with *B. megaterium*. For the other two bacteria, a 100 % effect was only obtained upon Triton X-100 addition to the cells in the presence of the peptides. Triton X-100 addition did cause a 100 % effect with all bacteria in the membrane depolarization assay. Another example of the higher sensitivity of this assay to relative minor membrane perturbations.The lysis buffer supplied with the BacTiter-Glo kit seemed to be an efficient way for bacterial cell lysis and was compatible with the membrane depolarization, where it gave the same results, and DAPI assays. However, it was not compatible with the Sytox-green assay as this led to significant quenching of the fluorescence.

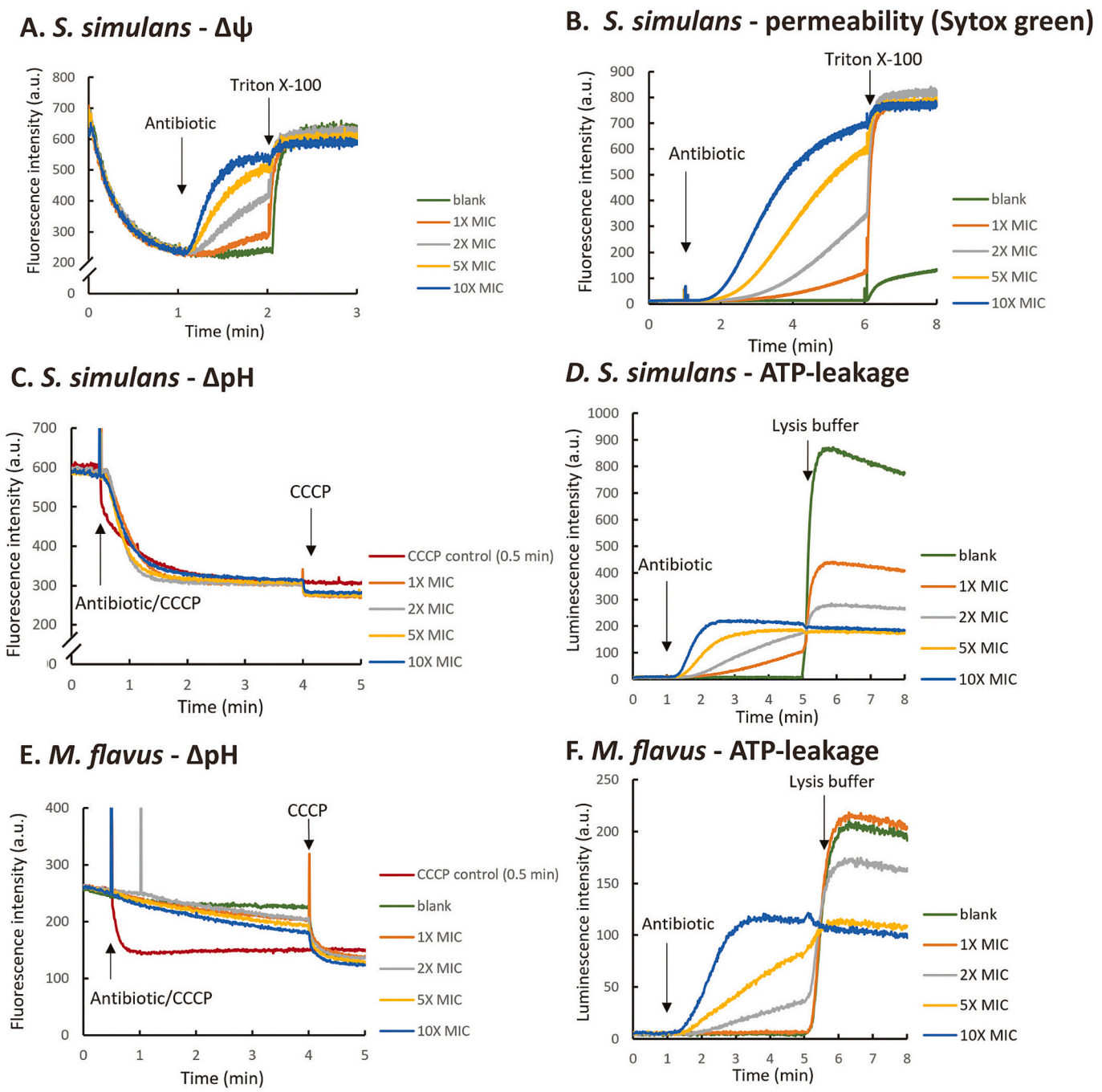

Fig. 1. Effects of nisin on the membranes of *S. simulans* and *M. flavus* determined using different fluorescent probes on (A) the membrane potential of *S. simulans*; (B) the membrane permeability of *S. simulans* determined using Sytox green; (C) the intracellular pH of *S. simulans*; (D) the intracellular ATP levels and leakage of ATP from *S. simulans*; (E) the intracellular pH of *M. flavus*; (F) the intracellular ATP levels and leakage of ATP from *M. flavus*. The addition of samples (antibiotics, TritonX-100, CCCP, Lysis buffer) is indicated by arrows. Different amounts of nisin which were equal to 1× MIC (orange), 2× MIC (grey), 5× MIC (yellow) and 10× MIC (blue) are indicated by different color. Blank and CCCP control trace are indicated by green and red. For each bacterium this was repeated twice, thus generating fully independent measurements. Experiment 1E was repeated three times.

0.5× MIC and 1× MIC do not appear to cause proton permeability in *M. flavus* (Fig. 2E). On the contrary, the signal has a clear increase, pointing to increased outflow protons from the cells.

In line with epilancin's bacteriostatic activity, it barely shows effects on membrane permeability in experiments using Sytox green, DAPI and luciferase (Figs. 2B and D, S3A, C and E). Only at high concentrations (5× & 10× MICs) some minor effects can be seen. Furthermore, although epilancin barely causes any ATP leakage from *S. simulans* or *M. flavus*, it did cause the internal ATP concentration to drop in both cells at the higher concentrations (Figs. 2D and S3E) albeit not to a large extent.

Previously, epilancin was predicted to kill bacteria via pore-formation in view of similarities between the structures of epilancin and nisin [47]. Our results show that this cannot be the case, at least not with respect to its activity towards *S. simulans* and *M. flavus*.

3.4. Epilancin 15× activity towards B. megaterium

Similar to what we observed for nisin, *B. megaterium* was also very sensitive to epilancin. It was clearly bactericidal as at 5× MIC it caused a

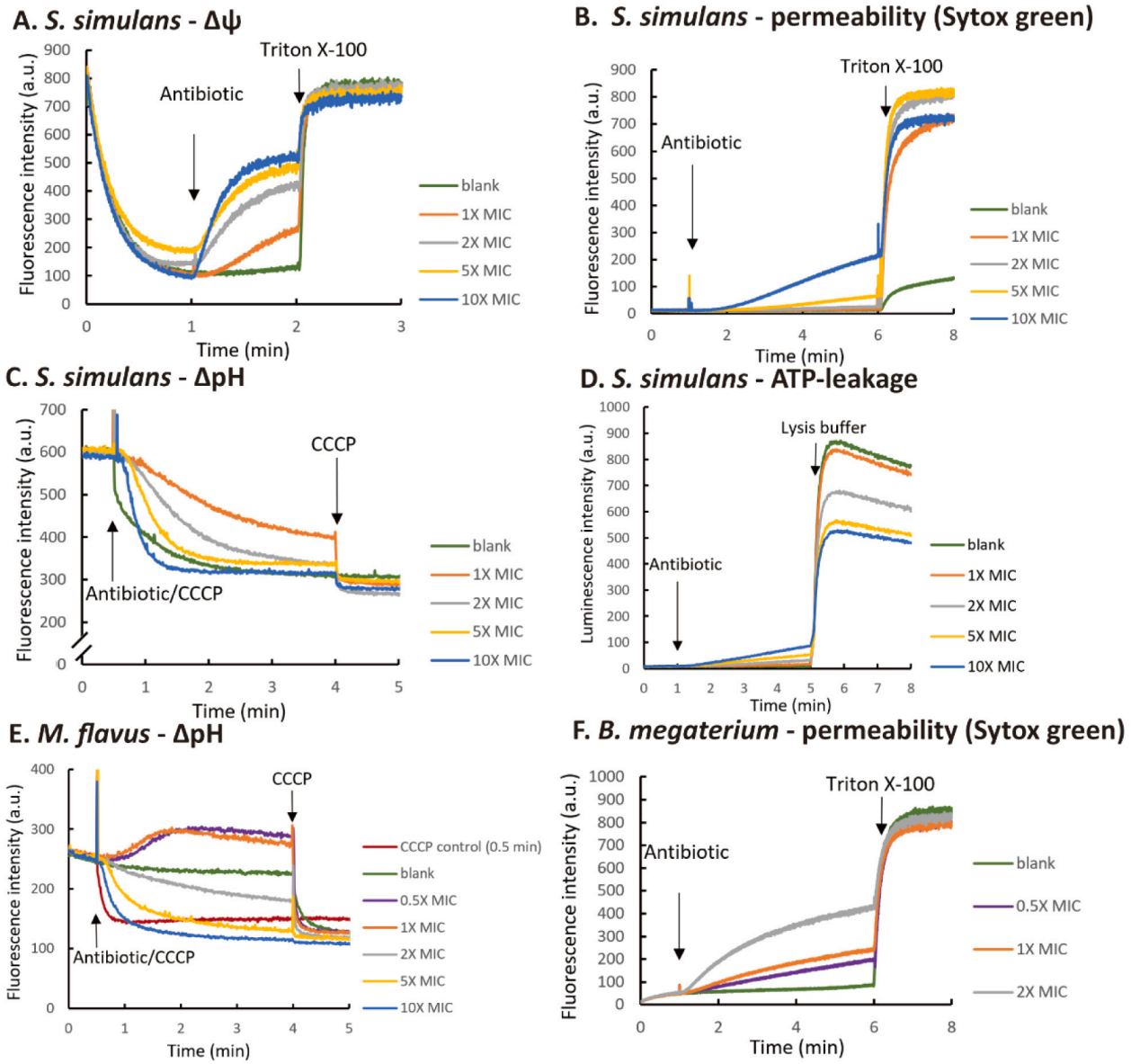

Fig. 2. Effects of epilancin 15× on the membrane of *S. simulans*, *M. flavus* and *B. megaterium* determined using different fluorescent probes on (A) the membrane potential of *S. simulans*; (B) the membrane permeability of *S. simulans* determined using Sytox green; (C) the intracellular pH of *S. simulans*; (D) the intracellular ATP levels and leakage of ATP from *S. simulans*; (E) the intracellular pH of *M. flavus*; (F) the membrane permeability of *B. megaterium* determined using Sytox green. The addition of samples (antibiotics, TritonX-100, CCCP, Lysis buffer) is indicated by arrows. Different amounts of epilancin 15× which were equal to 0.5× MIC (purple), 1× MIC (orange), 2× MIC (grey), 5XMIC (yellow) and 10× MIC (blue) are indicated by different color. Blank and CCCP control trace are indicated by green and red. For each bacterium this was repeated twice, thus generating fully independent measurements. Experiment 2E was repeated three times.

4-log reduction in cells after 5 min (Fig. P6). This high sensitivity was also reflected in the membrane depolarization assay, where epilancin, like nisin, showed membrane depolarization activity below its MIC value. At 0.1× MIC, epilancin exhibited already more than 50 % membrane depolarization in 2 min and effects were maximal at concentrations of 1× MIC or higher (Fig. S3F). The proton permeability assay showed similar results (Fig. S3H). Moreover, the Sytox green and DAPI assays indicated severe membrane damage at these higher concentrations (Figs. 2F and S3G) and these effects parallel the killing rates. Thus, these results suggest that the bactericidal activity of epilancin towards *B. megaterium* is mainly due to its membrane damaging effect.

3.5. *[R4L10]-teixobactin induced membrane permeabilization*

[R4L10]-teixobactin displayed a MIC value of 0.125 μg/mL (100 nM) which is 2-fold lower MIC than that of the natural version against MRSA ATCC 33591 [52]. Besides, it displays MICs in the range of 0.25–1 μg/mL (200–800 nM) against VRE, 0.03–0.5 μg/mL (24–400 nM) against MRSA, and 0.125–0.5 μg/mL (100–400 nM) against *Bacillus* spp. [52]. In this research, [R4L10]-teixobactin displayed MIC values equal to 1000 nM, 750 nM and 500 nM towards *S. simulans*, *M. flavus*, *B. megaterium* respectively. Thus, our MIC values were close to the range of MIC-values found in the literature even though we used a different method to determine them. The MIC values of [R4L10]-teixobactin towards our three test strains are 6–10 folds higher than that of nisin and epilancin 15×, therefore, to prevent possible a-specific effects due to high peptide concentrations, we only used concentrations equal to 1×, 2× and 5× the MICs of [R4L10]-teixobactin in our membrane disruption assays.

At lower [R4L10]-teixobactin concentrations (1× and 2× MIC), it barely killed *S. simulans* until at 5× MIC, the number of viable cells dropped with 90 % in 5 min (Fig. P7). Similar to the case of epilancin, [R4L10]-teixobactin only showed killing activity towards *S. simulans* at

the highest concentrations. The time killing assay indicated that [R4L10]-teixobactin should have a relatively low membrane perturbing activity compared to nisin, at least within the short time frame used here.

The membrane depolarization activity of [R4L10]-teixobactin towards *S. simulans* was in line with its low membrane-perturbing activity. Only at the highest concentration (5× MIC) a clear membrane depolarization effect could be observed and the maximal amount of dissipation that was reached in the experiment stayed below the 50 % (Fig. 3A). Similarly, the ΔpH was dissipated at concentrations higher than 1× MIC, with maximal effects only at a 5× MIC concentration (Fig. S4B). While similar results were observed in the DAPI assay (Fig. S4A), the Sytox green assay showed a different picture. A clear membrane permeability effect was observed already at 1× MIC and the maximal effect that was obtained at 5× MIC was above 70 % (Fig. 3B). In line with these results, [R4L10]-teixobactin induced ATP leakage, and a

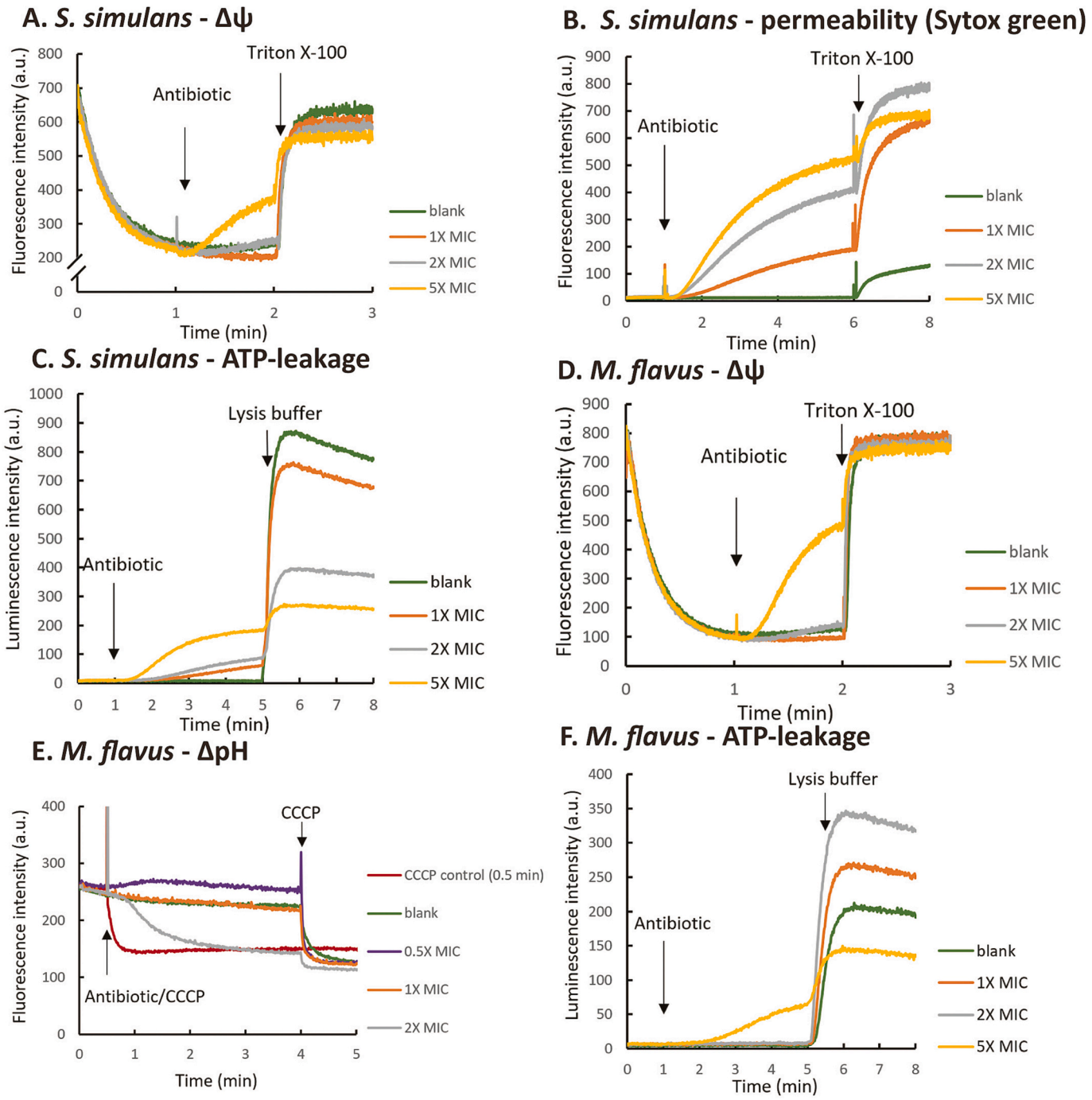

Fig. 3. Effects of [R4L10]-teixobactin on the membrane of *S. simulans* and *M. flavus* determined using different fluorescent probes on (A) the membrane potential of *S. simulans* determined using $DiSC_2(5)$; (B) the membrane permeability of *S. simulans* determined using Sytox green; (C) the ATP levels and leakage of ATP from *S. simulans*; (D) the membrane potential of *M. flavus*; (E) the intracellular pH of *M. flavus* determined, SE; (F) the ATP levels and leakage of ATP from *M. flavus*. The addition of samples (antibiotics, TritonX-100, Lysis buffer) is indicated by arrows. Different amounts of [R4L10]-teixobactin which were equal to 0.5× MIC (purple), 1× MIC (orange), 2× MIC (grey) and 5× MIC (yellow) are indicated by different color. Blank and CCCP control trace are indicated by green and red. For each bacterium this was repeated twice, thus generating fully independent measurements. Experiments 3E and 3F were repeated three times. (For interpretation of the references to color in this figure legend, the reader is referred to the web version of this article.)

low but significant amount of ATP was released from the cells at 1× MIC (Fig. 3C). Like nisin, a dual effect could be seen here as the cytosolic ATP concentration dropped significantly at concentrations equal to 2× and 5× MIC (Fig. 3C).

Similar to its activity towards *S. simulans*, [R4L10]-teixobactin killed 90 % of *M. flavus* cells in 5 min at a concentration equal to 5× MIC (Fig. P8). Likewise, its effects on the membrane potential (Fig. 3D) and ΔpH were also comparable (Fig. 3E) including the rise of the cellular pH at low concentrations of the peptide. No severe permeabilization could be observed at all concentrations in the Sytox assay and ATP only leaked out of the cells at the highest 5× MIC concentration (Figs. S4D and 3F). The DAPI results were (again) hardly showing any response with *M. flavus*, only some effect at 5× MIC could be observed (Fig. S4C). A very interesting effect could be observed for low concentrations (1 and 2× MIC) of [R4L10]-teixobactin on the internal ATP levels. A clear increase in total ATP levels of this bacterium could be observed, which we have never seen before in this test and seems unique for this combination of antibiotic and bacterial strain (Fig. 3F).

As observed for the other peptides, *B. megaterium* was more sensitive towards [R4L10]-teixobactin as well. More severe effects in the time-killing assay were paralleled by severe effects in the assays reporting on membrane permeabilization. [R4L10]-teixobactin at 2× MIC killed 3-log of cells in 5 min while at lower concentrations the effect was substantially lower in this time period (Fig. P9). In all membrane perturbation assays with *B. megaterium*, [R4L10]-teixobactin exhibited clear effects at 0.5× MIC and reached nearly 100 % at the concentration of 2× MIC (Fig. S4E–H).

3.6. The ultra-sensitivity of *B. megaterium* may be related to membrane lipid composition

What stood out in the experiments above was that the *B. megaterium* cells were very sensitive and rapidly killed by all three antibiotic peptides. This was always paralleled by severe membrane perturbation. To test if this may be caused by the membrane lipid composition of this strain compared to the other strains we determined their composition with respect to the acyl chain and headgroup. There were some differences observed in acyl chain composition between the three strains (Fig. S5). However, these small differences do likely not explain the high sensitivity of *B. megaterium* vs the other strains. This changed when the headgroup composition was determined (Fig. S6). Phosphatidylglycerol (PG) and cardiolipin (CL) were predominantly found in *S. simulans* and *M. flavus*, while phosphatidylethanolamine (PE) could only be observed for *B. megaterium*. Most conspicuous was the absence of Lysyl-PG, a version of PG with a lysine attached making it the only known naturally occurring cationic lipid [57], in the *B. megaterium* abstract. Lysyl-PG is synthesized from PG and flopped to the outer monolayer of the plasma membrane by MprF, and is involved in resistance against positively charged AMPs [58]. *B. megaterium* lacks the gene encoding for MprF, which explains the absence of this lipid in the extracts. Therefore, it is tempting to speculate that this absence of Lysyl-PG causes *B. megaterium* to be highly sensitive to the membrane-disruptive effects of the AMPs from in this study.

4. Discussion

Fluorescent probes that can measure, somehow, the extent of membrane damage are often used for determining the mode of action of antimicrobial peptides or other antibiotic compounds. Depending on the probe used, moderate or more severe effects on the permeability barrier of the bacterial plasma membrane are measured. Here we used five different assays and three different bacterial strains and compared how they report on the mode of action of three different antimicrobial peptides. First we tested how the different assays report on the well-established mode of action of nisin, that together with Lipid II efficiently forms pores in target membranes. Then, we tested these systems on two other peptide antibiotics. One peptide with a so far unknown mode of action was the lantibiotic epilancin 15×. The mode of action of the other, the [R4L10] analog of teixobactin, also involves targeting Lipid II and, similar to nisin, it clusters into higher order oligomers in a Lipid II dependent way. Recently, natural teixobactin was shown to induce membrane disruption in conjunction to its assembly into higher order oligomers. Whether this is also the case for the [R4L10] analog was not known [50].

4.1. General considerations

Changes in the internal pH of the cell that we measured using 5(6)-CFDA, SE or in the trans-membrane potential measured by $DiSC_2(5)$ were considered as moderate membrane permeabilization effects as they report on leakage of protons into and of (mainly) potassium ions out of the cells respectively. More severe membrane effects we determined by measuring the leakage of DNA probes into, or ATP from the cells. For the latter we devised an on-line luciferase-based assay that is able to determine both the leakage of ATP from the cells as well as the remaining ATP pool left in the cytosol. The membrane potential and ΔpH are directly linked to the cell's ability to generate ATP [56]. Thus, these three assays are, in principle, connected. The two DNA-dye based assays differ in terms of the size of the dye where SYTOX-green (MW 600 g/mol) is more than twice the size of DAPI (MW 277 g/mol) and thus may report differently based on the severity of the membrane perturbation. We have no evidence of these probe interference by the peptides.

Data from the previous century on polymeric exclusion thresholds of Gram-positive cell walls indicated that this threshold is rather high (e.g. number average molecular weight, Mn = 30,000 to 57,000 for *B. megaterium* and Mn = 25,000 for *Micrococcus lysodeikticus*) [59]. Likely the *staphylococci* have similar thresholds. This fits nicely with more recent data on the architecture of Gram-positive cell walls of *B. subtilis* and *S. aureus* of which the smallest determined pore-size present at the inner side of the peptidoglycan layer was ~6 nm [60]. Thus, the different dyes are not expected to be affected by different cell wall architectures. Indeed, we haven't detected any evidence for different behavior of the dyes with the different bacterial strains.

We consider severe membrane perturbation as the fastest way to kill bacteria and we could clearly find a good correlation between the killing kinetics of nisin and the assays that report on severe membrane disruption. An existing correlation between killing kinetics and membrane permeabilization is important to draw proper conclusions on whether the mechanism of action involves membrane perturbation. However, it should be noted that it is impossible to immediately stop the killing of bacteria by nisin (or any other AMP) while determining the number of CFUs after treatment. The amount of viable cells will likely continue to drop to some extent after plating out and incubation overnight, leading to a possible over estimation of the killing rate, especially if the AMPs have fast killing kinetics. Additionally, it should be realized that the membrane permeability experiments are only “sensitive” for up to two log reductions in cell numbers, as they cannot discriminate between 99 % killing (2-log reduction) or 99.9 % killing (3-log reduction). Nevertheless, whenever we noticed a higher than 2-log reduction of cell numbers after 5 min, this always correlated with the occurrence of severe membrane disruption in the assays. We noticed that, in general, there seemed to be a specific order in which these membrane perturbation effects are occurring. The ion and proton gradients are the first to be dissipated. Often, within the first minute after addition on the AMPs maximal effects were seen in the assays that measured the ΔpH and ΔΨ, while ATP-leakage and the Sytox green signal only appeared after a lag time (usually 30 s to 1 min). Yet, only the Sytox, DAPI and ATP assays correlated with bacterial killing, which implies that the effect on the ΔpH and ΔΨ alone, although stress related, are not sufficient to conclude that AMP's (or other compound's) killing mode involves membrane perturbation.

4.2. Specific observations

4.2.1. Nisin

From a targeted pore-former such as nisin it is to be expected that, provided it is able to reach Lipid II in the target membrane, it will cause severe membrane disruption. The pore-size of the nisin-lipid II pore-complex, estimated to be of about 2 nm in diameter, would easily allow passage of ATP and the DNA probes used in this study [46]. This was indeed what we observed, as virtually all assays indicated fast and severe membrane effects. There were however two exceptions; the DAPI assay with *M. flavus* and the proton permeability assay with the same bacteria. In combination with *M. flavus*, the DAPI probe displayed strange behavior compared to Sytox green with all the peptides tested here. This suggests that this combination of probe and bacterium is for some reason not compatible, emphasizing the need for multiple probes and bacteria when testing membrane effects of AMPs and proper positive controls. Our observation that nisin didn't cause a rapid and full dissipation of the proton gradient in *M. flavus* even at very high (10 × MIC) concentrations was especially surprising in relation to the results obtained with the other probes that all show (at least some) membrane perturbation at 1–2 × MIC. The other two peptides did show dissipation of the ΔpH, which, together with the behavior of the control (CCCP), rule out that 5(6)-CFDA is, similar to DAPI, not compatible with *M. flavus*. We currently do not have a good explanation for this aberrant effect of nisin on the pH gradient in *M. flavus*.

4.2.2. Epilancin 15×

The mechanism of action of epilancin 15× appeared to be different for all the three test strains we used. It acted bactericidal towards *B. megaterium* and, in line with this, it clearly induced membrane permeabilization in all our experiments even at concentrations lower than the MIC. The clear effects in the Sytox green and DAPI assays indicate a severe membrane damaging effect in this bacterium, possibly involving pore-formation. In contrast, epilancin 15× acted bacteriostatic towards *S. simulans* and *M. flavus* and displayed severe membrane effects (Sytox green influx and ATP-leakage) at relative high concentrations only with *S. simulans*. While with most assays a similar activity could be observed with the two bacteria, *M. flavus* showed a surprising increase of the internal pH in the presence of low (0.5 and 1 × MIC) peptide concentrations. At these concentrations no drop in cellular ATP levels and only a small dissipation of the membrane potential could be detected. This picture suggests that epilancin 15× targets an ATP-consuming process, while also the ATP-synthesis is inhibited, which in turn decreases the influx of protons [61]. In the meantime, protons are still pumped out of the cells by the respiratory chain. These effects together led to the increase of the cellular pH [62].

The inhibition of ATP-synthesis is most likely the result of the epilancin-induced dissipation of the membrane potential, the main determinant of the activity of the ATP-synthase [63–65]. Because bacteria maintained a ΔpH (which even increased at low concentrations) this suggests that the membrane is still intact. Therefore, the dissipation of the membrane potential is unlikely caused by a direct effect on the bilayer lipids of *M. flavus*, but may rather involve perturbation of the ion homeostasis in another way. A direct effect on ion transporters cannot be ruled out.

4.2.3. [R4L10]-teixobactin

The binding mode of [R4L10]-teixobactin to Lipid II in bacterial membranes was elucidated recently. The C-terminal depsi-cycle of teixobactin binds the pyrophosphate and MurNAc parts of Lipid II whereupon it assembles into antiparallel β-sheets in the membrane [51]. This is followed by a slower formation of a supramolecular fibrillar structure. For natural teixobactin, this was recently also shown [50]. The multimeric structure of the natural form contains, like the [R4L10] variant a concentrated hydrophobic patch and displays curvature that results in local thinning of the membrane upon fibril formation, which was considered as the reason for teixobactin's ability to cause membrane permeabilization. The polyprenyl tails of Lipid II that are concentrated within the hydrophobic patch are proposed to also play an active role in the membrane perturbation [50]. Although the 10th amino acid *allo*-enduracididine of teixobactin is replaced by leucine in [R4L10]-teixobactin which reduces Lipid II binding affinity, the interaction of R4L10 teixobactin with Lipid II resembles that of natural teixobactin in these aspects [50,51]. Indeed, we could show with our assays that also [R4L10]-teixobactin was able to permeabilize bacterial membranes, albeit that the severity of this permeabilization depended on the strain tested.

Similar as was observed for epilancin 15×, [R4L10]-teixobactin displayed different behavior towards the three different indicator strains. Towards *B. megaterium*, killing was paralleled by membrane perturbations in all assays, suggesting that membrane perturbation is a major aspect of [R4L10]-teixobactin's mechanism of action towards this bacterium. While [R4L10]-teixobactin induced somewhat less severe membrane effects towards *S. simulans*, which were in line with previous results, *M. flavus* was not that sensitive to [R4L10]-teixobactin [50]. What again stood out with this bacterium was an increased intracellular pH at 0.5 × MIC, that was also observed for epilancin, albeit that the effect was less severe with the [R4L10]-teixobactin variant. Interestingly and contrasting the effects of epilancin on this bacterium, [R4L10]-teixobactin caused an increase in intracellular ATP at the lower concentrations. This suggests that at least one major ATP-consuming biosynthesis pathway has been stopped and that the ATP-synthase remained active. Inhibition of ATP-consumption in the cells is most likely caused by blocking peptidoglycan and wall teichoic acid biosynthesis pathways via binding of the teixobactin analog to the isoprenoid-based precursors [50,51]. The lack of effect on the membrane potential in these bacteria would explain that the ATP-synthase activity remains intact. Active ATP-synthesis would then explain the lesser effects on the internal pH at low concentrations (0.5 and 1.0 × MIC), as protons would be flowing back to the cytosol via the ATP-synthase.

5. Conclusions

In this research, we have developed an on-line ATP measurement which determines the extent of ATP leakage from the bacteria in time and the total amount of ATP remaining in the bacteria. The on-line ATP measurements combined with membrane potential depolarization assays and proton permeability assays reflect how antibiotics interfere with the intracellular homeostasis of the pH, ions and ATP, which are highly interconnected and regulated. These three assays combined form a very powerful tool to reveal antimicrobial mechanisms. In view of their connectedness, we recommend to always combine these three assays if membrane effects of AMPs or other compounds are studied.

Almost all assays were consistent with the mode of action of nisin as the typical example of a targeted pore-former. Yet, even for such a clear MOA, deviations were observed in certain assay-bacterium combinations. This points to the importance of using multiple assays and bacteria for (general) mode of action studies.

The different behavior of epilancin 15× to the three strains makes it difficult to propose one general mode of action for this peptide. This, together with the recently found antagonization of the activity of epilancin 15× by Lipid II and, to a lesser extent, DOPG [40], indicates the need for further investigation of epilancin's mechanism of action in relation to its possible target.

For [R4L10]-teixobactin it is clear that its primary target, like natural teixobactin, is Lipid II and other prenyl-pyrophosphate-linked precursors [49]. The interaction with Lipid II leads to the formation of supramolecular fibrillar structures on the target membrane [50]. Whether the formation of these fibrillar structures leads to membrane damaging effects seems to depend on the membrane lipid composition of the target strain that is tested.

Declaration of competing interest

The authors declare the following financial interests/personal relationships which may be considered as potential competing interests: Ishwar Singh reports financial support was provided by acknowledges the Innovate UK and Department of Health and Social Care (DHSC), UK and Rosetrees Trust. Xiaoqi Wang and Yang Xu reports financial support was provided by China Scholarship Council.

Data availability

Data will be made available on request.

Acknowledgements

X. Wang (201508330301) and Y. Xu (201606230222) were funded by the China Scholarship Council. I.S. acknowledges the Innovate UK and Department of Health and Social Care (DHSC), UK and Rosetrees Trust for their kind support (SBRI grant 106368-623146 and Rosetrees Trust grant CF-2021-2\102). The views expressed in this publication are those of the authors and not necessarily those of Innovate UK or DHSC, UK.

Appendix A. Supplementary data

Supplementary data to this article can be found online at https://doi.org/10.1016/j.bbamem.2023.184160.

References

[1] W.C. Wimley, K. Hristova, Antimicrobial peptides: successes, challenges and unanswered questions, J. Membr. Biol. 239 (2011) 27–34.
[2] K. Reddy, R. Yedery, C. Aranha, Antimicrobial peptides: premises and promises, Int. J. Antimicrob. Agents 24 (2004) 536–547.
[3] A.R. Koczulla, R. Bals, Antimicrobial peptides, Drugs 63 (2003) 389–406.
[4] K.A. Brogden, Antimicrobial peptides: pore formers or metabolic inhibitors in bacteria? Nat. Rev. Microbiol. 3 (2005) 238–250.
[5] Z. Oren, Y. Shai, Mode of action of linear amphipathic α-helical antimicrobial peptides, Pept. Sci. 47 (1998) 451–463.
[6] H.W. Huang, F.-Y. Chen, M.-T. Lee, Molecular mechanism of peptide-induced pores in membranes, Phys. Rev. Lett. 92 (2004), 198304.
[7] K. Matsuzaki, in: K. Matsuzaki (Ed.), Antimicrobial Peptides. Advances in Experimental Medicine and Biology, 1117, Springer, Singapore, 2019. https://doi.org/10.1007/978-981-13-3588-4_2.
[8] K. Lohner, New strategies for novel antibiotics: peptides targeting bacterial cell membranes, Gen. Physiol. Biophys. 28 (2009) 105–116.
[9] R.M. Epand, R.F. Epand, Bacterial membrane lipids in the action of antimicrobial agents, J. Pept. Sci. 17 (2011) 298–305.
[10] H.H. Haukland, H. Ulvatne, K. Sandvik, L.H. Vorland, The antimicrobial peptides lactoferricin B and magainin 2 cross over the bacterial cytoplasmic membrane and reside in the cytoplasm, FEBS Lett. 508 (2001) 389–393.
[11] L.T. Nguyen, E.F. Haney, H.J. Vogel, The expanding scope of antimicrobial peptide structures and their modes of action, Trends Biotechnol. 29 (2011) 464–472.
[12] D. Gidalevitz, Y. Ishitsuka, A.S. Muresan, O. Konovalov, A.J. Waring, R.I. Lehrer, K. Y. Lee, Interaction of antimicrobial peptide protegrin with biomembranes, Proc. Natl. Acad. Sci. U. S. A. 100 (2003) 6302–6307.
[13] V.C. Kalfa, H.P. Jia, R.A. Kunkle, P.B. McCray Jr., B.F. Tack, K.A. Brogden, Congeners of SMAP29 kill ovine pathogens and induce ultrastructural damage in bacterial cells, Antimicrob. Agents Chemother. 45 (2001) 3256–3261.
[14] M.E. Falagas, S.K. Kasiakou, Colistin: the revival of polymyxins for the management of multidrug-resistant gram-negative bacterial infections, Clin. Infect. Dis. 40 (2005) 1333–1341.
[15] N.W. Schmidt, G.C.L. Wong, Antimicrobial peptides and induced membrane curvature: geometry, coordination chemistry, and molecular engineering, Curr. Opinion Solid State Mater. Sci. 17 (2013) 151–163.
[16] N.P. Chongsiriwatana, J.S. Lin, R. Kapoor, M. Wetzler, J.A.C. Rea, M.K. Didwania, C.H. Contag, A.E. Barron, Intracellular biomass flocculation as a key mechanism of rapid bacterial killing by cationic, amphipathic antimicrobial peptides and peptoids, Sci. Rep. 7 (2017) 16718.
[17] E. Breukink, I. Wiedemann, C. Van Kraaij, O. Kuipers, H.-G. Sahl, B. De Kruijff, Use of the cell wall precursor lipid II by a pore-forming peptide antibiotic, Science 286 (1999) 2361–2364.
[18] I.J. Galván Márquez, B. McKay, A. Wong, J.J. Cheetham, C. Bean, A. Golshani, M. L. Smith, Mode of action of nisin on Escherichia coli, Can. J. Microbiol. 66 (2020) 161–168.
[19] H. Rottenberg, The measurement of membrane potential and deltapH in cells, organelles, and vesicles, Methods Enzymol. 55 (1979) 547–569.
[20] A. Peña, S. Uribe, J.P. Pardo, M. Borbolla, The use of a cyanine dye in measuring membrane potential in yeast, Arch. Biochem. Biophys. 231 (1984) 217–225.
[21] A.P. Singh, P. Nicholls, Cyanine and safranine dyes as membrane potential probes in cytochrome c oxidase reconstituted proteoliposomes, J. Biochem. Biophys. Methods 11 (1985) 95–108.
[22] G. Milligan, P.G. Strange, Reduction in accumulation of [3H] triphenylmethylphosphonium cation in neuroblastoma cells caused by optical probes of membrane potential: evidence for interactions between carbocyanine dyes and lipophilic anions, Biochim. Biophys. Acta, Mol. Cell Res. 762 (1983) 585–592.
[23] A.S. Waggoner, Dye indicators of membrane potential, Annu. Rev. Biophys. Bioeng. 8 (1979) 47–68.
[24] G. Cabrini, A.S. Verkman, Localization of cyanine dye binding to brush-border membranes by quenching of n-(9-anthroyloxy) fatty acid probes, Biochim. Biophys. Acta 862 (1986) 285–293.
[25] P.J. Sims, A.S. Waggoner, C.-H. Wang, J.F. Hoffman, Mechanism by which cyanine dyes measure membrane potential in red blood cells and phosphatidylcholine vesicles, Biochemistry 13 (1974) 3315–3330.
[26] S.J.B.J. Krasne, in: Interactions of Voltage-sensing Dyes With Membranes. I. Steady-state Permeability Behaviors Induced by Cyanine Dyes 30, 1980, pp. 415–439.
[27] S. Krasne, Interactions of voltage-sensing dyes with membranes. II. Spectrophotometric and electrical correlates of cyanine-dye adsorption to membranes, Biophys. J. 30 (1980) 441–462.
[28] P. Breeuwer, J. Drocourt, F.M. Rombouts, T. Abee, A novel method for continuous determination of the intracellular pH in bacteria with the internally conjugated fluorescent probe 5 (and 6-)-carboxyfluorescein succinimidyl Ester, Appl. Environ. Microbiol. 62 (1996) 178–183.
[29] S.C. Kuo, J.O. Lampen, Osmotic regulation of invertase formation and secretion by protoplasts of Saccharomyces 106 (1971) 183.
[30] G.Y. Lomakina, Y.A. Modestova, N.N. Ugarova, Bioluminescence assay for cell viability, Biochemistry. Biokhimiia 80 (2015) 701–713.
[31] B.L. Roth, M. Poot, S.T. Yue, P.J. Millard, Bacterial viability and antibiotic susceptibility testing with SYTOX green nucleic acid stain, Appl. Environ. Microbiol. 63 (1997) 2421.
[32] M. Yasir, D. Dutta, M.D.P. Willcox, Comparative mode of action of the antimicrobial peptide melimine and its derivative Mel4 against Pseudomonas aeruginosa, Sci. Rep. 9 (2019), 7063-7063.
[33] R. Rathinakumar, W.F. Walkenhorst, W.C. Wimley, Broad-spectrum antimicrobial peptides by rational combinatorial design and high-throughput screening: the importance of interfacial activity, J. Am. Chem. Soc. 131 (2009) 7609–7617.
[34] C. Pérez-Peinado, S.A. Dias, M.M. Domingues, A.H. Benfield, J.M. Freire, G. Rádis-Baptista, D. Gaspar, M.A.R.B. Castanho, D.J. Craik, S.T. Henriques, A.S. Veiga, D. Andreu, Mechanisms of bacterial membrane permeabilization by crotalicidin (Ctn) and its fragment Ctn(15–34), antimicrobial peptides from rattlesnake venom, J. Biol. Chem. 293 (2018) 1536–1549.
[35] A.W. Coleman, M.J. Maguire, J.R. Coleman, Mithramycin- and 4'-6-diamidino-2-phenylindole (DAPI)-DNA staining for fluorescence microspectrophotometric measurement of DNA in nuclei, plastids, and virus particles, J. Histochem. Cytochem. 29 (1981) 959–968.
[36] M.L. Mangoni, N. Papo, D. Barra, M. Simmaco, A. Bozzi, A.Di Giulio, A.C.J.B. J. Rinaldi, in: Effects of the Antimicrobial Peptide Temporin L on Cell Morphology, Membrane Permeability and Viability of Escherichia coli 380, 2004, pp. 859–865.
[37] M. Urfer, J. Bogdanovic, F.L. Monte, K. Moehle, K. Zerbe, U. Omasits, C.H. Ahrens, G. Pessi, L. Eberl, J.A. Robinson, in: A Peptidomimetic Antibiotic Targets Outer Membrane Proteins and Disrupts Selectively the Outer Membrane in *Escherichia coli* 291, 2016, pp. 1921–1932.
[38] B. Chudzik, M. Koselski, A. Czuryło, K. Trębacz, M. Gagoś, A new look at the antibiotic amphotericin B effect on Candida albicans plasma membrane permeability and cell viability functions, Eur. Biophys. J. 44 (2015) 77–90.
[39] C. Chatterjee, M. Paul, L. Xie, W.A. van der Donk, Biosynthesis and mode of action of lantibiotics, Chem. Rev. 105 (2005) 633–684.
[40] X. Wang, Q. Gu, E. Breukink, Non-lipid II targeting lantibiotics, Biochim. Biophys. Acta Biomembr. 1862 (2020), 183244.
[41] E. Breukink, H.E. van Heusden, P.J. Vollmerhaus, E. Swiezewska, L. Brunner, S. Walker, A.J. Heck, B. de Kruijff, Lipid II is an intrinsic component of the pore induced by nisin in bacterial membranes, J. Biol. Chem. 278 (2003) 19898–19903.
[42] H.E. Hasper, B. de Kruijff, E. Breukink, Assembly and stability of Nisin−Lipid II pores, Biochemistry 43 (2004) 11567–11575.
[43] H.E. van Heusden, B. de Kruijff, E. Breukink, Lipid II induces a transmembrane orientation of the pore-forming peptide lantibiotic nisin, Biochemistry 41 (2002) 12171–12178.
[44] I. Wiedemann, E. Breukink, C. van Kraaij, O.P. Kuipers, G. Bierbaum, B. de Kruijff, H.-G. Sahl, Specific binding of nisin to the peptidoglycan precursor lipid II combines pore formation and inhibition of cell wall biosynthesis for potent antibiotic activity, J. Biol. Chem. 276 (2001) 1772–1779.
[45] J. Medeiros-Silva, S. Jekhmane, A.L. Paioni, K. Gawarecka, M. Baldus, E. Swiezewska, E. Breukink, M. Weingarth, High-resolution NMR studies of antibiotics in cellular membranes, Nat. Commun. 9 (2018) 3963.
[46] I. Wiedemann, R. Benz, H.-G. Sahl, Lipid II-mediated pore formation by the peptide antibiotic nisin: a black lipid membrane study, J. Bacteriol. 186 (2004) 3259.
[47] J.E. Velásquez, X. Zhang, W.A. Van Der Donk, Biosynthesis of the antimicrobial peptide epilancin 15X and its N-terminal lactate, Chem. Biol. 18 (2011) 857–867.
[48] M.B. Ekkelenkamp, M. Hanssen, S.-T. Danny Hsu, A. de Jong, D. Milatovic, J. Verhoef, N.A.J. van Nuland, Isolation and structural characterization of

epilancin 15X, a novel lantibiotic from a clinical strain of Staphylococcus epidermidis, FEBS Lett. 579 (2005) 1917–1922.
[49] L.L. Ling, T. Schneider, A.J. Peoples, A.L. Spoering, I. Engels, B.P. Conlon, A. Mueller, T.F. Schäberle, D.E. Hughes, S. Epstein, M. Jones, L. Lazarides, V. A. Steadman, D.R. Cohen, C.R. Felix, K.A. Fetterman, W.P. Millett, A.G. Nitti, A. M. Zullo, C. Chen, K. Lewis, A new antibiotic kills pathogens without detectable resistance, Nature 517 (2015) 455–459.
[50] R. Shukla, F. Lavore, S. Maity, M.G.N. Derks, C.R. Jones, B.J.A. Vermeulen, A. Melcrová, M.A. Morris, L.M. Becker, X. Wang, R. Kumar, J. Medeiros-Silva, R.A. M. van Beekveld, A. Bonvin, J.H. Lorent, M. Lelli, J.S. Nowick, H.D. MacGillavry, A.J. Peoples, A.L. Spoering, L.L. Ling, D.E. Hughes, W.H. Roos, E. Breukink, K. Lewis, M. Weingarth, Teixobactin kills bacteria by a two-pronged attack on the cell envelope, Nature 608 (2022) 390–396.
[51] R. Shukla, J. Medeiros-Silva, A. Parmar, B.J.A. Vermeulen, S. Das, A.L. Paioni, S. Jekhmane, J. Lorent, A. Bonvin, M. Baldus, M. Lelli, E.J.A. Veldhuizen, E. Breukink, I. Singh, M. Weingarth, Mode of action of teixobactins in cellular membranes, Nat. Commun. 11 (2020) 2848.
[52] A. Parmar, R. Lakshminarayanan, A. Iyer, V. Mayandi, E.T. Leng Goh, D.G. Lloyd, M.L.S. Chalasani, N.K. Verma, S.H. Prior, R.W. Beuerman, A. Madder, E.J. Taylor, I. Singh, Design and syntheses of highly potent teixobactin analogues against Staphylococcus aureus, methicillin-resistant Staphylococcus aureus (MRSA), and vancomycin-resistant enterococci (VRE) in vitro and in vivo, J. Med. Chem. 61 (2018) 2009–2017.
[53] A.D. Paiva, E. Breukink, H.C. Mantovani, Role of lipid II and membrane thickness in the mechanism of action of the lantibiotic bovicin HC5, Antimicrob. Agents Chemother. 55 (2011) 5284–5293.
[54] A.J.F. Egan, R. Maya-Martinez, I. Ayala, C.M. Bougault, M. Banzhaf, E. Breukink, W. Vollmer, J.-P. Simorre, Induced conformational changes activate the peptidoglycan synthase PBP1B, Mol. Microbiol. 110 (2018) 335–356.
[55] H.-G. Sahl, H. Brandis, Production, purification and chemical properties of an antistaphylococcal agent produced by Staphylococcus epidermidis, Microbiology 127 (1981) 377–384.
[56] P.C. Maloney, E.R. Kashket, T.H. Wilson, A protonmotive force drives ATP synthesis in bacteria, Proc. Natl. Acad. Sci. 71 (1974) 3896.
[57] R. Rashid, M. Veleba, K.A. Kline, Focal targeting of the bacterial envelope by antimicrobial peptides, Front. Cell Dev. Biol. 4 (2016) 55.
[58] L. Friedman, J.D. Alder, J.A. Silverman, Genetic changes that correlate with reduced susceptibility to daptomycin in Staphylococcus aureus, Antimicrob. Agents Chemother. 50 (2006) 2137–2145.
[59] R. Scherrer, P. Gerhardt, Molecular sieving by the bacillus megaterium cell wall and protoplast, J. Bacteriol. 107 (1971) 718–735.
[60] L. Pasquina-Lemonche, J. Burns, R.D. Turner, S. Kumar, R. Tank, N. Mullin, J. S. Wilson, B. Chakrabarti, P.A. Bullough, S.J. Foster, J.K. Hobbs, The architecture of the gram-positive bacterial cell wall, Nature 582 (2020) 294–297.
[61] I.L. Bartek, M.J. Reichlen, R.W. Honaker, R.L. Leistikow, E.T. Clambey, M. S. Scobey, A.B. Hinds, S.E. Born, C.R. Covey, M.J. Schurr, A.J. Lenaerts, M. I. Voskuil, Antibiotic bactericidal activity is countered by maintaining pH homeostasis in Mycobacterium smegmatis, mSphere 1 (2016).
[62] V.R.I. Kaila, M. Wikström, Architecture of bacterial respiratory chains, Nat. Rev. Microbiol. 19 (2021) 319–330.
[63] G. Kaim, P. Dimroth, ATP synthesis by the F1Fo ATP synthase of Escherichia coli is obligatorily dependent on the electric potential, FEBS Lett. 434 (1998) 57–60.
[64] G. Kaim, P. Dimroth, Voltage-generated torque drives the motor of the ATP synthase, EMBO J. 17 (1998) 5887–5895.
[65] G. Kaim, P. Dimroth, ATP synthesis by F-type ATP synthase is obligatorily dependent on the transmembrane voltage, EMBO J. 18 (1999) 4118–4127.